Assessing the feasibility for Atmosphere-Ocean Coupling of JMA's Global Ensemble Prediction System

TAKAKURA Toshinari[1,*], OCHI Kenta[1], ADACHI Yukimasa[2] and KOMORI Takuya[1]
1: Numerical Prediction Division, Japan Meteorological Agency
2: Meteorological Research Institute, Japan Meteorological Agency
E-mail: t-takakura@met.kishou.go.jp

1. Introduction

The Global Ensemble Prediction System (GEPS) operated by the Japan Meteorological Agency (JMA) incorporates an atmospheric model with a two-tiered sea surface temperature (SST) approach (Takakura and Komori 2020) for lower boundary conditions. This technique indirectly represents atmosphere-ocean interaction by combining SSTs prescribed as persisting anomalies from climatological SSTs and SSTs operationally precomputed using JMA's seasonal EPS. In the work reported here, feasibility for atmosphere-ocean coupling of GEPS was assessed toward the incorporation of more directly representative atmosphere-ocean interaction.

2. Experimental design

(1) Retrospective forecast experiments

Retrospective forecast experiments covering winter 2019/20 and summer 2020 were conducted with focus on initial shocks caused by inconsistencies between the lower boundary specifications of the atmospheric model in coupling prediction and atmospheric analysis representing initial conditions. Only a control member was run, and the forecast time was limited to 264 hours. The first experiment (CNTL) was conducted using the currently operational GEPS (Yamaguchi et al. 2022). In the next experiment (CPL), atmosphere-ocean coupling was applied to CNTL using an ocean model with specifications similar to those of the seasonal EPS (JMA/MRI-CPS3; Kubo and Ochi 2022). In the last experiment (CPL2), mixed land-ocean-lake grid and sea-ice coupling were switched off to reduce the initial shocks seen in CPL. Furthermore, tendency coupling (e.g., Mogensen et al. 2017) was applied to SSTs at mid- and high latitudes in CPL2 up to 132 hours and linear relaxation to full coupling was applied from 132 to 264 hours by adding the tendency of the SST in the ocean model to SST analysis values.

(2) 30-year (1991 – 2020) hindcast experiments

Hindcast experiments for CNTL, CPL and CPL2 were conducted with the same specifications as Sekiguchi et al. (2022), except for an ensemble size of 5, a forecast time up to 438 hours and initial dates of three days for each of summer and winter.

3. Results

Figure 1 shows the initial shocks of CPL and CPL2 against CNTL in the root mean square error (RMSE) differences of zonal mean temperature with lead times of 24 hours in the retrospective forecast experiments. The larger RMSE in the lower atmosphere of CPL presumably resulted from differences in SST, sea-ice and mixed land-ocean-lake grid specifications between coupling prediction and atmospheric analysis. CPL2 exhibited reduced deterioration in RMSE at high latitudes via the switching off of the mixed land-ocean-lake grid and sea-ice coupling and at mid-latitudes due to tendency coupling effects.

To evaluate the impact of tendency coupling, anomaly correlation coefficients (ACCs) of SSTs were compared over week 1 of the hindcast experiment (Figure 2). ACCs in CPL were better in the tropics and the summer hemisphere than those of CNTL, but worse in mid-latitude eddy-rich oceanic regions. The deterioration in these regions is attributed to inadequate representation of meso-scale ocean eddies in the ocean model with 0.25-degree resolution. Meanwhile, CPL2 exhibited reduced deterioration in the mid-latitudes because the high spatial variability of SST analysis is maintained in tendency coupling. As a result, the bias-corrected ACCs of CPL2 were superior to those of CNTL for many atmospheric scores in the hindcast experiments (Figure 3). ACC without bias correction also shows better scores except for 850 hPa temperatures in the Tropics, where there is an influence from the cold SST bias of the coupled model (not shown). Overall, including the improved Madden-Julian Oscillation (MJO) forecast skill contributed by better atmospheric circulation (Figure 4), the CPL2 results are promising for further GEPS development.

References

Kobayashi, S., Y. Kosaka, J. Chiba, T. Tokuhiro, Y. Harada, C. Kobayashi, and H. Naoe, 2021: JRA-3Q: Japanese reanalysis for three quarters of a century. *WCRP-WWRP Symposium on Data Assimilation and Reanalysis/ECMWF annual seminar 2021*, WMO/WCRP, O4-2, https://symp-bonn2021.sciencesconf.org/data/355900.pdf.

Kubo Y., and K. Ochi, 2022: Verification of JMA/MRI-CPS3 and JMA Global Ensemble Prediction System in the sub-seasonal forecast. *WGNE Res. Activ. Earth Sys. Modell*., submitted.

Matsueda, M., and H. Endo, 2011: Verification of medium-range MJO forecasts with TIGGE. *Geophys. Res. Lett*., **38**, L11801.

Merchant, C.J., Embury, O., Roberts-Jones, J., Fiedler, E., Bulgin, C.E., Corlett, G.K., Good, S., McLaren, A., Rayner, N., Morak-Bozzo, S. and Donlon, C. (2014), Sea surface temperature datasets for climate applications from Phase 1 of the European Space Agency Climate Change Initiative (SST CCI). *Geosci. Data J*., **1**, 179-191.

Mogensen, K.S., L. Magnusson and J-R. Bidlot, 2017: Tropical Cyclone Sensitivity to Ocean Coupling *ECMWF Technical Memorandum*, **794**.

Sekiguchi, R., Y. Ichikawa, K. Ochi, and T. Takakura, 2022: Hindcast verification of JMA's GEPS for one-month prediction. *WGNE Res. Activ. Earth Sys. Modell*., submitted.

Takakura, T., and T. Komori, 2020: Two-tiered sea surface temperature approach implemented to JMA's Global Ensemble Prediction System. *WGNE. Res. Activ. Earth Sys. Modell.*, **50**, 6.15-6.16.

Yamaguchi, H., Y. Ichikawa, T. Iwahira, Y. Kuroki, C. Matsukawa, R. Nagasawa, K. Ochi, R. Sekiguchi, T. Takakura, M. Ujiie, and H. Yonehara, 2022: Upgrade of JMA's Global Ensemble Prediction System. *WGNE Res. Activ. Earth Sys. Modell.*, submitted.

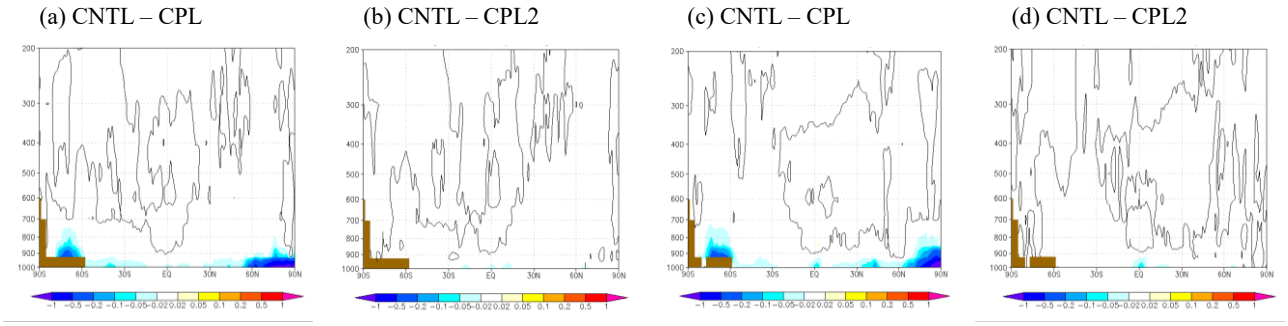

Figure 1 Root mean square error (RMSE) differences against JMA's global analysis in zonal mean temperature (K) at lead times of 24 h in retrospective forecast experiments for (a), (b) winter and (c), (d) summer. Black lines indicate a zero RMSE difference.

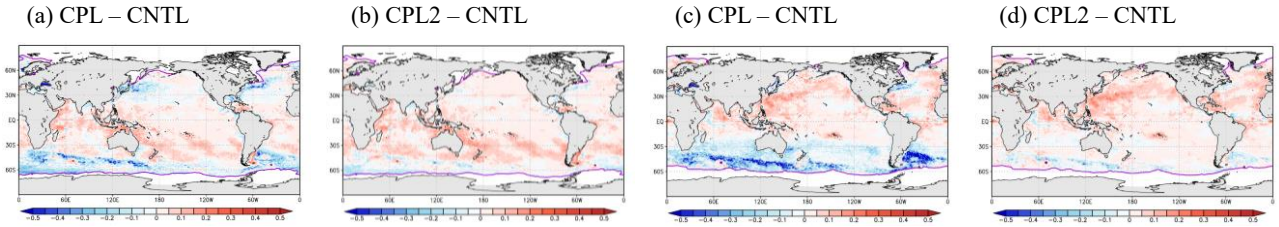

Figure 2 Anomaly correlation coefficient (ACC) differences of ensemble-mean SST over week 1 against ESA SST CCI (Merchant et al. 2014) for (a), (b) winter and (c), (d) summer. The verification period is 1991 – 2015. Areas of sea-ice presence are masked, with purple lines indicating mask boundaries.

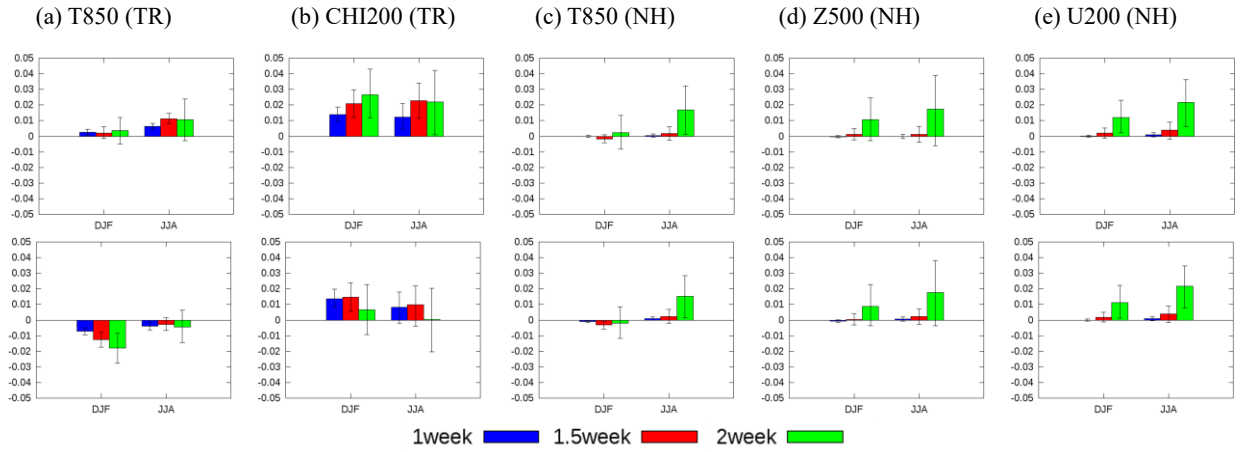

Figure 3 Anomaly correlation coefficient (ACC) differences (top) with bias correction and (bottom) without bias correction for winter (DJF) and summer (JJA). (a) and (b) are in the Tropics (TR; 20°S－20°N), and (c), (d) and (e) are in the Northern Hemisphere (NH; 20－90°N). Each figure shows (a), (c) 850-hPa temperature, (b) 200-hPa velocity potential (d) 500-hPa height and (e) 200-hPa zonal wind. Positive values represent ACCs of CPL2 exceeding those of CNTL. Error bars indicate two-sided 95% confidence levels. ACCs are calculated against JRA-3Q (Kobayashi et al. 2021) for the period from 1991 to 2020.

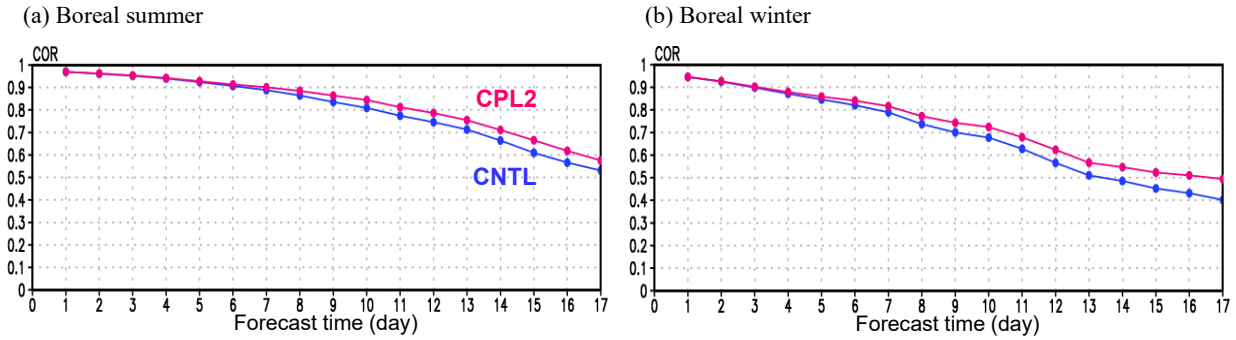

Figure 4 Correlation of MJO index (Matsueda and Endo 2011) in (a) boreal winter and (b) boreal summer. The red and blue lines represent results for CPL2 and CNTL, respectively. The verification period is 1991 – 2020.